Nigerian Journal of Science and Environment 2024 Volume 22 (2) 28 – 50 ISSN: 3043 – 4440
https://doi.org/10.61448/njse222243

KINETIC, ISOTHERM AND THERMODYNAMIC STUDIES OF THE ADSORPTION OF CRESOL RED DYE USING AGRICULTURAL WASTES

[*1]Ogundiran, A. A., [2]Ogundiran, O. O., [1]Badeji, A. A. and [1]Osinubi A. D.
[1]Department of Chemical Sciences, Tai Solarin University of Education, Ijagun, Ogun State
[2]Department of Chemistry, Sikiru Adetona College of Education, Science and Technology Omu-Ajose, Ogun State
*Correspondence author's email: ogundiranaa@tasued.edu.ng ; Telephone: +2347066709187

Abstract

Agricultural wastes and plant biomass are alternative low-cost adsorbents because they can be used without or with a minimum processing. In the present study, batch experiments were carried out to study the adsorption of cresol red (CR) unto mango leaf (ML) and orange peel (OP). Several parameters that affect adsorption process such as pH, adsorbent dosage, contact time, initial dye concentration and temperature were investigated. FTIR and SEM were used to determine the functional group responsible for adsorption. The results revealed that the highest adsorption efficiency was at pH 5 for the two adsorbents. It was also discovered that CR removal efficiency increased with the increase in contact time and adsorbent dosage while adsorption capacity was higher with increase in initial dye concentration but removal efficiency was lowered. The kinetics conform with the pseudo-first-order kinetic model for mango leaf but conform with the pseudo-second-order kinetic for orange mesocarp due to the value of the correlation coefficient (R^2). Based on the value of correlation coefficient, the experimental results for the removal by mango leaf best fitted the Langmuir isotherm model with monolayer adsorption capacity of 70.64 mg. g^{-1}, while Freundlich isotherm model was best fitted to the experimental results for the adsorption of CR by Orange peel. The thermodynamic results revealed that the process is spontaneous and endothermic.

Keywords: adsorption, dye, kinetic, thermodynamic, isotherm

Introduction

In the past decades, the utilization of synthetic dyes has increased drastically thereby increasing the challenges posed by pollution of the environment by colored wastewater. Effluents of various industries like textile, distillery, paint, finishing, pharmaceutical, food, leather, natural and synthetic dyes, paper and pulp industries and oil mills etc. are the major contributors of water pollution (Kumar *et. al.,* 2020). Dyes are toxic to animals and humans' life

even at a low concentration (Stjepanović *et. al.,* 2021) because of their recalcitrant and persistent nature in the environment. Most dyes are carcinogenic and mutagenic in nature which will consequently pose serious negative health effect on human and animals (Aquino *et. al.,* 2014; Khatri *et. al.,* 2018). The presence of dyes in water bodies and the environment may inhibit the process of photosynthesis by water plants and also reduce the amount of dissolved oxygen due to blockage of sunlight from penetrating into the aquatic environments (Kouba and Zhuang,1994; Moussavi and Mahmoudi, (2009); Qin *et. al.,* (2009); Donia *et. al.,* (2009)].

Adsorption compared with several techniques such as photocatalytic degradation (Joseph *et. al.,* 2009), membrane filtration (Zhu *et. al.,* 2017), precipitation (Gündüz and Bayrak, 2017), ion exchange (Reynier *et. al.,* 2015) that have been employed to remove wastewater contaminants has proven to be the most efficient (Ogundiran *et. al.,* (2022); Ofudje *et. al.,* 2022). Recently, adsorption has gained more attentions due to the simplicity in its design, cost effectiveness, ease of operation and efficacy.

The utilization of agricultural waste materials has been investigated as low cost adsorbents for the removal of contaminants from wastewater (Bhatnagar *et. al.,* 2015). Agricultural wastes are very abundant and less costly under most circumstances and they are biodegradable. Thus, they can be converted into low-cost adsorbents for water contaminant remediation. The alternative application of these wastes also solves a solid-waste disposal problem in the environment. There are now several examples of the raw agricultural wastes that have successfully removed a myriad of water contaminants, some of the agricultural waste materials that have been employed in past studies include sunflower seed shells (Malik, 2003), sawdust (Malik, 2003), palm oil fibre (Darus e*t. al.,* 2005), cotton plant wastes (Tunç *et. al.,* 2009), soya bean waste (Kooh *et. al.,* 2016), coffee waste (Lafi *et. al.,* 2019), banana peel (Oyekanmi *et. al.,* 2019), marula seed husk

(Edokpayi *et. al.,* 2019), macadamia seed husk (Mutunga *et, al.,* 2020), pepper stalk (Barour *et. al.,* 2023), and litchi seed (Edokpayi and Makete, 2021).

The purpose of the present study was to assess the adsorption capacities of mango leaf and orange peel for the removal of the Cresol red dye in a batch experiment under different parameter.

Materials and methods

Preparation of Adsorbents

The adsorbents orange peel (OP) and mango leaf (ML) were collected at the market at Ijebu-ode. The samples (OP and ML) were first washed with tap water, repeated with distilled water to remove any impurities adhering to the surface and then the samples were cut into pieces and oven-dried at 105 ^{o}C overnight. The dried samples were grounded and sieved through 30-mesh to get a consistent size of adsorbent powder. The fine powders of these agricultural wastes were then preserved in plastic bags for use as adsorbents.

Preparation of Cresol Red Solution

The stock solution of Cresol Red (CR) was prepared by dissolving 1.0 g of dye in 1000 mL of distilled water. Then from the stock solution, experimental solution of different concentration 50, 100, 150, 200 mg/L and 250mg/L were prepared by serial dilution process of initial stock solution into 100 mL of distilled water. The pH values of dye solutions were adjusted using 0.1 M HCl or NaOH to the required value and measured using a pH meter

Adsorbent characterization

FTIR spectra were used to investigate the functional groups of the adsorbents, and each adsorbent was loaded as KBr discs and recorded in a Fourier Transform Infrared Spectrophotometer

Batch Adsorption studies

Batch adsorption experiments were performed with 250 mL flasks, 20 mL dye solution was taken into 250 mL flask and was shaken at 250 rpm till the equilibrium in a temperature regulated water bath shaker. Each experiment was performed by keeping one parameter as a variable while keeping others constant in other to optimize

the parameters. 20 mL dye solution was brought in contact with the adsorbents at varying operation condition. The contact time was varied from (0 -140) min, adsorbent dose (0.2 -1.0) g, pH (2-6), temperature (25- 45) ℃ and adsorbate concentration (50-250) mg/L. After equilibrium was attained, each sample was centrifuged to separate adsorbent from the dye solution. The supernatant was analysed with a UV-Vis spectrophotometer (Hitachi, U3210, Japan) at a maximum wavelength (λmax)

The adsorption data of the orange mesocarp and mango peel on cresol red obtained from UV-Visible spectrophotometer were calculated to determine the Cresol Red removal rate (%) and adsorption capacity (mg/g). The formulas of calculation are as follow:

$$\text{Removal rate (\%)} = \frac{C_o - C_e}{C_o} x\ 100 \quad (1)$$

$$\text{Adsorption Capacity (A)} = (C_o - C_e)\frac{V}{M} \quad (2)$$

Where A (mg/g) is the dye adsorption capacity, C_o (mg/L) and Ce (mg/L) is respectively the initial and equilibrium dye concentrations in the solution, V (L) is the solution volume, and M (g) is the mass of adsorbent.

Kinetic study

The Lagergren pseudo-first-order and pseudo-second-order kinetic models were used to predict the adsorption of cresol red in this study. The linearized expressions for the pseudo-first-order kinetic model and pseudo-second-order kinetic are shown in the equations below (Lagergren, (1898); Ho and McKay (1999); Revellame *et. al.*, (2020):

$$ln(q_e - q_t) = lnq_e - K_1 t \quad (3)$$

where qe and qt (mg/g) are the adsorption capacities at equilibrium and at time t (min), respectively, and K_1 is the adsorption rate constant (min^{-1}). The intercept and slope of the plot of $ln(q_e - q_t)$ versus t, respectively, were used to estimate the values of q_e and K_1.

The pseudo-second-order equation is given by the following equation:

$$\frac{1}{q_t} = \frac{1}{K_2 q_e^2} + \frac{1}{q_e t} \quad (4)$$

where K_2 is the corresponding adsorption rate constant (mg/g·min)

Thermodynamic Study

Thermodynamic parameters for the adsorption of CR with both adsorbents were calculated using the van't Hoff equation (Lima et al 2020). In particular, the changes of entropy (ΔS^0), enthalpy (ΔH^0), and free energy (ΔG^0) of the adsorption on OP and ML were calculated using the equations below:

$$\Delta G^0 = \Delta H^0 - T\Delta S^0 \qquad (5)$$

$$\Delta G = -RTInk \qquad (6)$$

$$Ink = {\Delta S}/{R} + {\Delta H}/{RT} \qquad (7)$$

where R (8.3145 J $mol^{-1}K^{-1}$) stands for ideal gas constant, K (Lg^{-1}) is equilibrium constant and T (K) is the absolute temperature. The changes in the free energy (ΔG°, kJ/mol) values were calculated from Equation 5 above.

Isothermal studies

In the present experiment, Langmuir and Freundlich isothermal models were used to study the equilibrium characteristics of the adsorption of CR**.**

The Langmuir linear equation is commonly expressed as followed (Langmuir, 1916):

$$\frac{C_e}{qe} = \frac{1}{K_L Q_{max}} + \frac{C_e}{Qmax} \qquad (8)$$

where Ce is the equilibrium concentration of the dye (CR) (mg/L), q_e is the quantity of CR dye sorbed at equilibrium (mg/g), Q_{max} is the maximum amount sorbed (mg/g), and K_L is the Langmuir sorption constant (L/mg). A plot of Ce versus Ce/qe was linear showing the applicability of Langmuir adsorption isotherm for cresol red adsorption

The Freundlich isotherm model is given by (Freundlich,1906):

$$Inq_e = InK_F + \frac{1}{n}InC_e \qquad (9)$$

where qe is the quantity of dye sorbed at equilibrium (mg/g), Ce is the equilibrium concentration of dye in solution (mg/L). A plot of lnCe versus lnq_e was linear, where K_F is measure of adsorption capacity (mg/g) and n is adsorption intensity (Edokpayi *et. al.,* 2015).

Results and Discussion

Characterization of adsorbent

The adsorbents were characterized by Fourier-transform infrared spectroscopy (FT-IR) technique to determine the different functional groups of the adsorbents. FT-IR spectra of the OM and ML before and after adsorption were obtained within the spectral range of 4000-450 cm^{-1} shown in (Fig. 1) below. The peak around 3415.66 cm^{-1} showed the presence of hydroxyl group(-OH) and N-H group stretching vibrations. The presence of aliphatic groups ($–CH_2$ or $–CH_3$) was proved by the peaks at 2925.96 cm^{-1} and 2841.65cm^{-1} due to the stretching vibrations of C–H bonds (Qian *et.al.*, 2018). The peak at 1644.57 and 1633.59 cm^{-1} for OP and ML respectively shows the presence of C=O bond from carbonyls and to C=C present in the aromatic rings. The characteristics band at 1023.57 cm^{-1} for OP and 1022.7 cm^{-1} for ML corresponds to alcoholic C–O bond (Kanakarajua *et. al.*, 2018). After the sorption of the dye by the adsorbents, the spectra showed a decrease in absorbance bands when compared to the absorption bands before adsorption of cresol red. The reduction of absorbance peaks suggested that the available sites of the sorbent had been occupied by CR dye. Similar result was reported by (Elavarasan *et. al.*, (2018); Jegede *et. al.*, 2021).

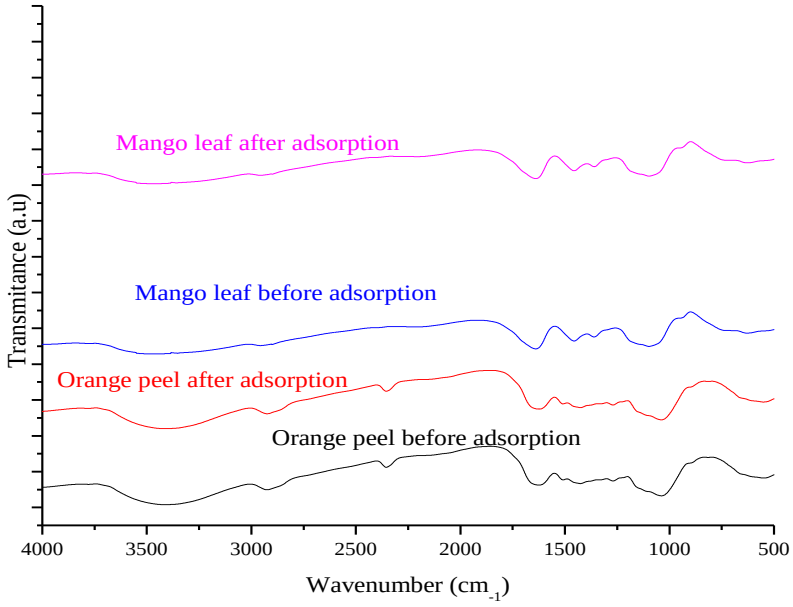

Figure 1: FTIR Spectra of orange peel and mango leaf.

Effect of solution pH

The pH of the medium is one of the most important parameters in adsorption study. Therefore, influence of solution pH on cresol red uptake was evaluated within pH range between 2–6. The result as shown in figure 2 depict that the adsorption of the dye was affected by the pH of the solution. As the pH increased the percentage of dye removed from solution also increased, this continue until pH 5 where the percentage removal of dye was optimal for both the adsorbents that is 88% for OP and 73% for MP. At low pH the surface of the adsorbents was positively charged due to more positive ions in the solution which caused the low percentage removal of the dye from the solution (Yagub *et. al.*, 2014). Increasing the pH value from 5 to 6 resulted in relative low uptake in dye absorption capacity, as shown in Figure 2. This may be due to the negative charge of the biomass surface as the pH rises (pH >5), thereby reducing the interaction of dye with adsorbent surface because of electrostatic repulsion (Demirbas and Nas (2009); Chiou and Li (2002).

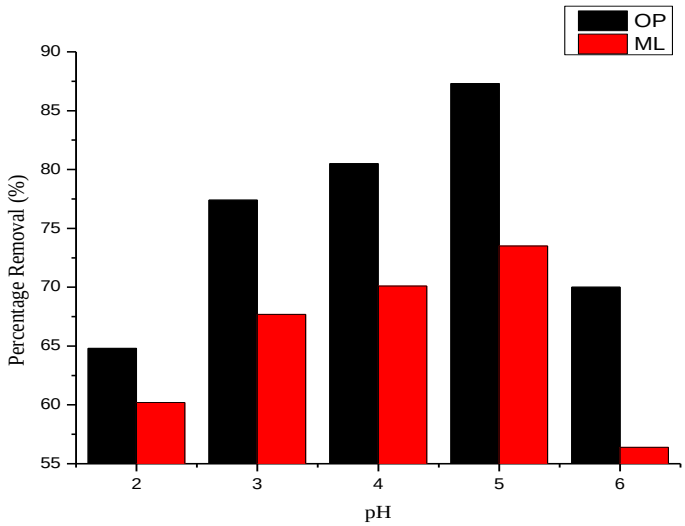

Figure 2: Effect of pH on percentage removal of Cresol red adsorption

Effect of initial concentration and contact time on the biosorption capacity

To determine the biosorption equilibrium time, the batch adsorption process was

carried out at different contact times and the different initial concentrations. Figure 1 showed the interaction between contact time and initial concentration on the adsorption capacities of the adsorbents for the removal of cresol red dye. The results indicate that the adsorption of the dye increased as its concentration increased with longer time of adsorption. The adsorption capacities of the adsorbents increased with increase in the time of adsorption. At the early stages of the process there was a rapid removal of the dye which may be due to the available number of sites on the adsorbents for adsorption (de Souza *et. al.*, 2022), but as the reaction proceeds the rate of the dye uptake reduced as the equilibrium was reached due to the increased number of adsorption sites that have been occupied. This similar observation was also reported by Hamad and Saied (2021); Ogundiran *et. al.*, (2022). The maximum amount of dye was removed at contact time of 80 mins and 100 mins by OP and ML respectively, the adsorption capacity increased with increasing the dye concentration but the percentage removal of dye decreased.

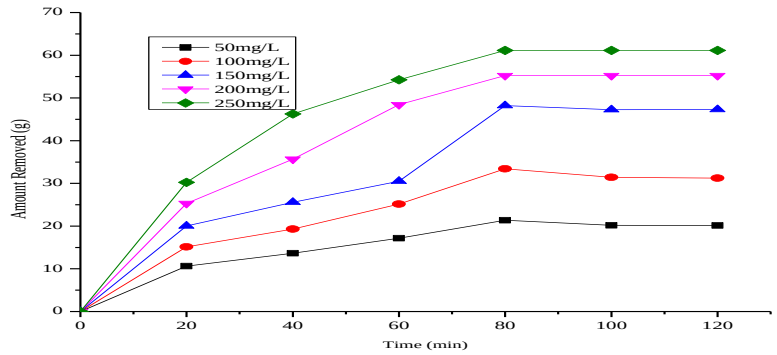

Figure 3: Effect of initial dye concentration and contact time on the removal CR onto OP

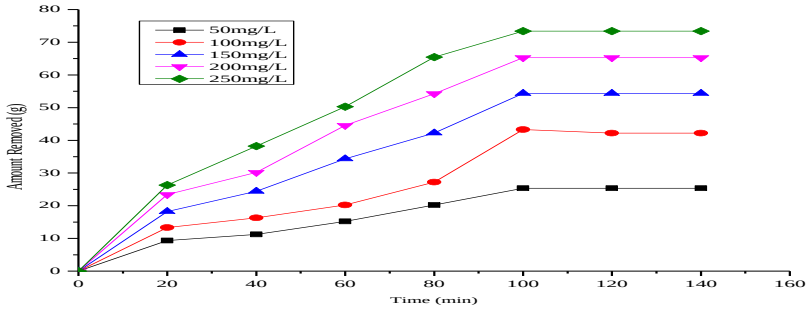

Figure 4: Effect of initial dye concentration and contact time on the removal CR onto ML

Effect of Adsorbent dosage

Study of the effect of adsorbent dosage gives an idea of the effectiveness of an adsorbent and the ability of a dye to be adsorbed with a minimum dosage, so as to identify the ability of an adsorbent from an economical point of view. Figure 3. shows the removal of cresol red dye at different adsorbent doses (0.2 – 1.0 g). It can be depicted that the percentage of dye removed is directly proportional to the adsorbent dosage. The percent sorbate removed increased from 47.5% to 66.5% for OP and 50.35 % to 69.35 % for ML as the adsorbent dosage increased from 0.2 to 0.8 g. The increase in percentage of dye removed with increasing adsorbent dosages is due to increase in the number of sorption active sites at the adsorbent surface with increasing the dose (Ghaedi *et. al.*, 2011). But the sorption capacity decreased at the further increment in biosorbent dosage to 1 g. This may be due to overcrowding of adsorbent particles (Abe *et. al.*, 2019; Ogundiran *et. al.*, 2022).

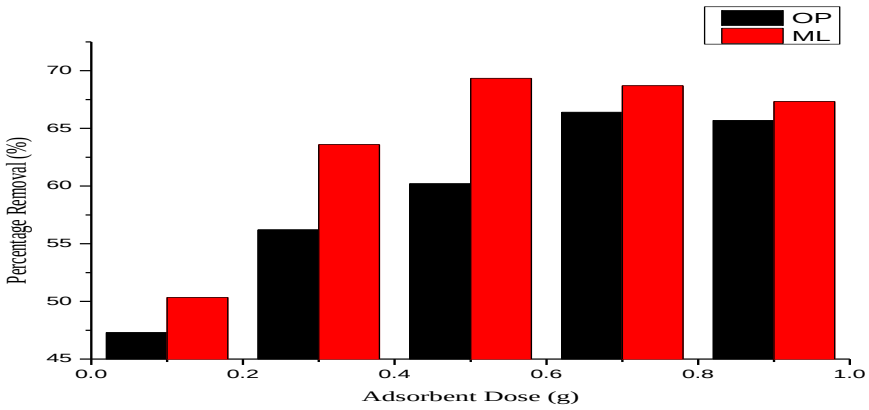

Figure 5: Effect of adsorbent dose on the uptake of cresol red

Kinetic of adsorption

The kinetic studies for the removal of CR were carried out as a function of time of contact at different initial concentration of the dye solution. Two kinetic models were used for this study, they are pseudo first order and pseudo second order kinetics.

Table 2 showed the values of parameters and correlation coefficients (R^2) obtained from the calculation from the kinetic models. The parameter calculated for the PSO kinetic model has a higher R^2 (correlation coefficient) than the PFO model for the removal of CR by OP. In addition, the calculated amount of dye adsorbed (q_e) values from the pseudo-second-order kinetic model were closer to the experimental values than that of the pseudo-first-order model. Therefore, the adsorption reaction followed pseudo second order kinetic model for orange peel as an adsorbent while the rate of adsorption followed pseudo first order for mango leaf as an adsorbent for all the time interval and the rate constant were affected by initial concentration of the dye. The PFO kinetic model assumes that the rate of adsorbate removal changes with time.

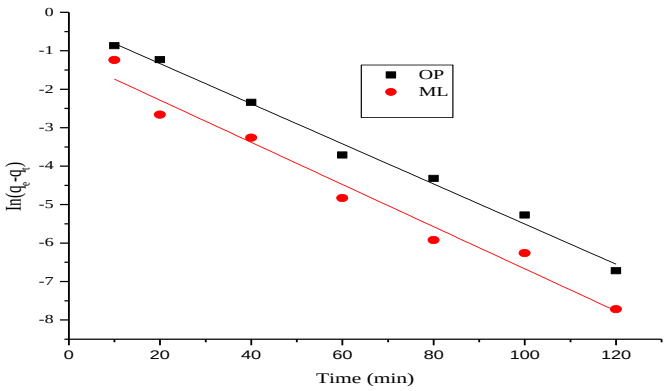

Figure 6: Pseudo-first order adsorption kinetic plot for adsorption of cresol red dye

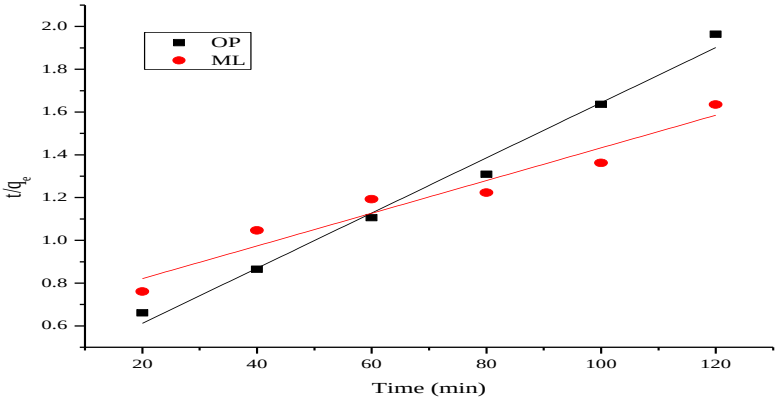

Figure 7: Pseudo-second order adsorption kinetic plot for adsorption of cresol red dye.

Adsorption isotherms

Isotherm study shows how the adsorbate interacts with the adsorbents during the adsorption process (Sharma *et. al.*, 2019). Langmuir and Freundlich models were used for the present study. The isotherm plots for CR dye adsorption on the adsorbents are shown in figures 5 and 6 while isotherm parameters obtained are given in the Table 2 below. According to the table, the correlation coefficient (R^2) for the Langmuir model was found to be better in predicting the adsorption of CR onto ML (0.977) compared to that of the Freundlich (0.898). This indicates that CR dye molecules created a monolayer coverage with homogenous distribution on the outer surface of the mango leaf. While for

adsorption of CR onto OP, Freundlich has a better fit with R^2 (0.998) than Langmuir isotherm (0.958), which indicated that the surface of OP was not uniform and had almost heterogeneous sites for CR dye adsorption.

The value of R_L calculated from Langmuir isotherm is between 0 and 1. This value was higher than zero, indicating that the adsorption of CR onto OP was favorable under the condition studied (Lim *et. al.*, 2017; Bayram *et. al.*, 2022). Also, the value of adsorption intensity ($^1/_n$) gotten from Freundlich isotherm was below 1 indicated a favorable adsorption of the dye on OP (Feng *et. al.*, 2021; Hashem *et. al.*, 2021).

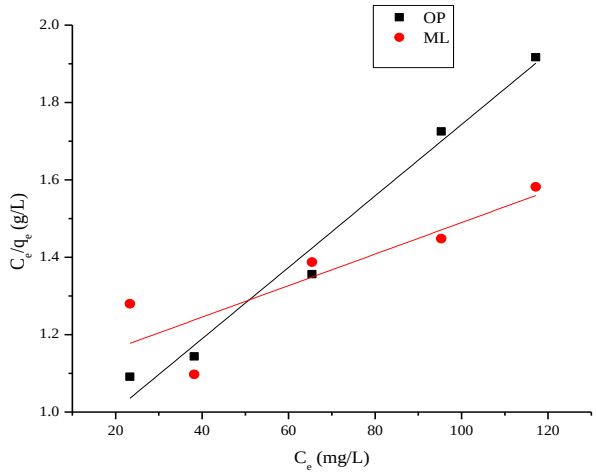

Figure 8: Langmuir isotherm plot for adsorption of cresol red dye

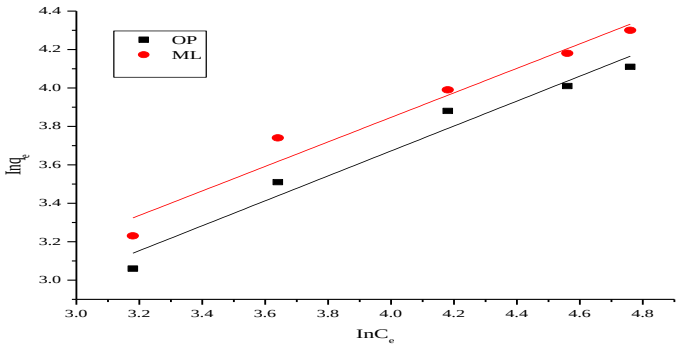

Figure 9: Freundlich isotherm plot for adsorption of cresol red dye

Effect of Temperature and Thermodynamic studies

The adsorption cresol red dye was studied at varied temperature, Figure 4 represents the effect of temperature on CR adsorption onto OP and ML at different temperatures. The percentage of CR dye uptake increased with the increase in solution temperature from 25–45 °C, which is an indication that the uptake of the dye by the adsorbents is endothermic in nature. Increase in the adsorption of the CR by adsorbents may be due to enhancement of the available active sites on the adsorbents and increased mobility of the adsorbate as the temperature increased (Ahmad *et. al*., 2015).

The summary of respective thermodynamic parameters ΔG^o, ΔH^o, and ΔS^o for the adsorption of CR are presented in Table 4. The values of Gibbs free energies (ΔG^o) were negative, indicating the adsorption of CR on the adsorbents were both spontaneous and feasible, the process does not need an external source for it to occur. The enthalpy change (ΔH^o) values were positive at various temperatures. The adsorption of CR was endothermic because the activation of dye molecules at the aligned sites occurred as a result of temperature increase. The positive values of entropy change (ΔS^o) indicated less randomness in their structural arrangement (Olu-Owolabi *et. al.*, 2009).

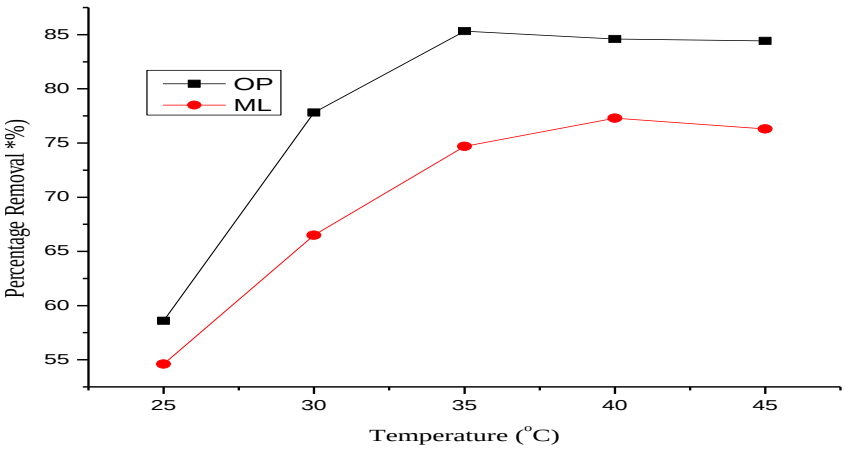

Figure 10: effect of temperature on the uptake of cresol red

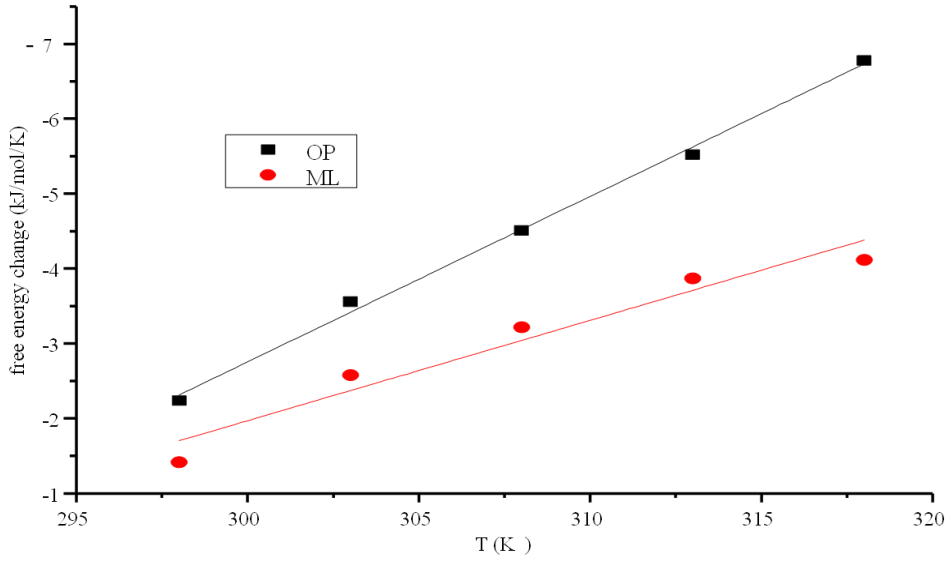

Figure 11: The free energy plot for the adsorption of cresol red using OP and ML

Conclusion

Orange peel and mango leaf were utilized as potential sorbents for the sequestration of Cresol Red dye. The process of adsorption was favored by acidic pH of 5 and contact time of 80 mins for OP and 100 mins for ML. Pseudo-second-order kinetic model and Freundlich isotherm model provided the best fit sorption process by OP while pseudo first order kinetic and Langmuir isotherm was best fit for the sorption of CR with ML. The adsorption of CR was feasible, spontaneous and endothermic process for both adsorbents. Characterization of the sorbents revealed the nature, active sites, and functional groups present on the sorbents. It can be concluded that the orange peel and mango leaf which are cheap and easily accessible materials were found to be very effective for the removal of cresol red from aqueous solutions.

Competing Interest

There is no competing interest to declare.

References

Abe, F. R., Machado, A. L., Soares, A. M., de Oliveira, D. P., & Pestana, J. L. (2019). Life history and behavior effects of synthetic and

natural dyes on Daphnia magna. *Chemosphere*, 236, 124390.

Ahmad, M. A., Ahmad, N., & Bello, O. S. (2015). Modified durian seed as adsorbent for the removal of methyl red dye from aqueous solutions. *Applied Water Science*, 5, 407-423.

Aquino, J. M., Rocha-Filho, R. C., Ruotolo, L. A., Bocchi, N., & Biaggio, S. R. (2014). Electrochemical degradation of a real textile wastewater using β-PbO2 and DSA® anodes. *Chemical Engineering Journal*, 251, 138-145

Barour, M., Tounsadi, H., Khnifira, M., Farnane, M., Machrouhi, A., Abdennouri, M., & Barka, N. (2023). Adsorption of dyes on microwave assisted activated stalks of pepper plants: Experimental, DFT and Monte Carlo simulation studies. *Applied Surface Science Advances*, *1*6, 100424.

Bayram, O., Köksal, E., Göde, F., & Pehlivan, E. (2022). Decolorization of water through removal of methylene blue and malachite green on biodegradable magnetic Bauhinia variagata fruits. *International Journal of Phytoremediation*, 24(3), 311-323.

Bhatnagar, A., Sillanpää, M., & Witek-Krowiak, A. (2015). Agricultural waste peels as versatile biomass for water purification–A review. *Chemical Engineering Journal*, 270, 244-271.

Chiou, M. S., & Li, H. Y. (2002). Equilibrium and kinetic modeling of adsorption of reactive dye on cross-linked chitosan beads. *Journal of Hazardous Materials*, 93(2), 233-248.

Darus, F. M., Hashim, H. J., Laiman, R., & Yusoff, M. N. (2005). Use of palm oil fiber, an agricultural waste for removal of methylene blue from aqueous solution. In Proceeding Seminar Kebangsaan Pengurusan

Persekitaran 4–5 July, *UKM, Bangi*, 301-308.

de Souza, C. C., de Souza, L. Z. M., Yılmaz, M., de Oliveira, M. A., da Silva Bezerra, A. C., da Silva, E. F., ... & Machado, A. R. T. (2022). Activated carbon of Coriandrum sativum for adsorption of methylene blue: Equilibrium and kinetic modeling. *Cleaner Materials*, 3, 100052.

Demirbas, E., & Nas, M. Z. (2009). Batch kinetic and equilibrium studies of adsorption of Reactive Blue 21 by fly ash and sepiolite. *Desalination*, 243(1-3), 8-21.

Donia, A. M., Atia, A. A., Al-Amrani, W. A., & El-Nahas, A. M. (2009). Effect of structural properties of acid dyes on their adsorption behavior from aqueous solutions by amine modified silica. *Journal of Hazardous Materials*, 161(2-3), 1544-1550.

Edokpayi, J. N., & Makete, E. (2021). Removal of Congo red dye from aqueous media using Litchi seeds powder: Equilibrium, kinetics and thermodynamics. *Physics and Chemistry of the Earth, Parts A/B/C*, 123, 103007.

Edokpayi, J. N., Ndlovu, S. S., & Odiyo, J. O. (2019). Characterization of pulverized Marula seed husk and its potential for the sequestration of methylene blue from aqueous solution. *BMC Chemistry*, 13(1), 10.

Edokpayi, J. N., Odiyo, J. O., Popoola, E. O., Alayande, O. S., & Msagati, T. A. (2015). Synthesis and characterization of biopolymeric chitosan derived from land snail shells and its potential for Pb2+ removal from aqueous solution. *Materials*, 8(12), 8630-8640.

Elavarasan, A., Chitradevi, S., Nandhakumar, V., Sivajiganesan, S., & Kadhiravan, S. (2018). FT-IR spectra, XRD and EDX studies on the adsorption of methylene blue

dye present in aqueous solution onto acid activated carbon prepared from Mimusops elengi leaves. *Journal of applied chemistry*, 11(7), 51.

Feng, S., Du, X., Bat-Amgalan, M., Zhang, H., Miyamoto, N., & Kano, N. (2021). Adsorption of REEs from aqueous solution by EDTA-chitosan modified with zeolite imidazole framework (ZIF-8). *International Journal of Molecular Sciences*, 22(7), 3447.

Freundlich, H. M. F. Z. (1906). Adsorption in solids. *Z. Phys. Chem*, 57, 385-470.

Ghaedi, M., Ramazani, S., & Roosta, M. (2011). Gold nanoparticle loaded activated carbon as novel adsorbent for the removal of Congo red. *Indian Journal of Science and Technology*, 1208-1217.

Gündüz, F., & Bayrak, B. (2017). Biosorption of malachite green from an aqueous solution using pomegranate peel: equilibrium modelling, kinetic and thermodynamic studies. *Journal of Molecular Liquids*, 243, 790-798.

Hamad, M. T., & Saied, M. S. (2021). Kinetic studies of Congo red dye adsorption by immobilized Aspergillus niger on alginate. *Applied Water Science*, 11, 1-12.

Hashem, A., Aniagor, C. O., Taha, G. M., & Fikry, M. (2021). Utilization of low-cost sugarcane waste for the adsorption of aqueous Pb (II): kinetics and isotherm studies. *Current Research in Green and Sustainable Chemistry*, 4, 100056.

Ho, Y. S., & McKay, G. (1999). Pseudo-second order model for sorption processes. *Process biochemistry*, 34(5), 451-465.

Jegede, M. M., Durowoju, O. S., & Edokpayi, J. N. (2021). Sequestration of hazardous dyes from aqueous solution using raw and modified agricultural waste.

Adsorption Science & Technology, 1-21.

Joseph, O., Rouez, M., Métivier-Pignon, H., Bayard, R., Emmanuel, E., & Gourdon, R. (2009). Adsorption of heavy metals on to sugar cane bagasse: Improvement of adsorption capacities due to anaerobic degradation of the biosorbent. *Environmental Technology*, 30(13), 1371-1379.

Kanakarajua, D., Rusydah, N., Shahdada, M., Limb, Y., & Pace, A. (2018). Magnetic hybrid TiO2/Alg/FeNPs triads for the efficient removal of methylene blue from water. *Sustainable Chemistry and Pharmacy* 8, 50–62

Khatri, J., Nidheesh, P. V., Singh, T. A., & Kumar, M. S. (2018). Advanced oxidation processes based on zero-valent aluminum for treating textile wastewater. *Chemical Engineering Journal*,348, 67-73.

Kooh, M. R. R., Dahri, M. K., Lim, L. B., Lim, L. H., & Malik, O. A. (2016). Batch adsorption studies of the removal of methyl violet 2B by soya bean waste: isotherm, kinetics and artificial neural network modelling. *Environmental Earth Sciences*, 75, 1-14.

Kouba J.F. & Zhuang P., (1994). Color removal for textile dyeing wastewater. *Fluid/Particle Separation Journal*. 7, 87-90

Kumar, P.; Rehab, H.; Hegde, K.; Brar, S.K.; Cledon, M.; Kermanshahi-Pour, A.; Duy, S.V.; Sauvé, S.; & Surampalli, R.Y. (2020). Physical and biological removal of Microcystin-LR and other water contaminants in a biofilter using Manganese Dioxide coated sand and Graphene sand composites. *Science of the Total Environment*, 703, 135052.

Lafi, R., Montasser, I., & Hafiane, A. (2019). Adsorption of congo red dye from aqueous solutions by

prepared activated carbon with oxygen-containing functional groups and its regeneration. *Adsorption Science & Technology*, 37(1-2), 160-181.

Lagergren, S. (1898). About the theory of so-called adsorption of solution substances.

Langmuir, I. (1916). The constitution and fundamental properties of solids and liquids. Part I. Solids. *Journal of the American Chemical Society*, 38(11), 2221-2295.

Lim, L. B., Priyantha, N., Tennakoon, D. T. B., Chieng, H. I., Dahri, M. K., & Suklueng, M. (2017). Breadnut peel as a highly effective low-cost biosorbent for methylene blue: equilibrium, thermodynamic and kinetic studies. *Arabian Journal of Chemistry*, 10, S3216-S3228.

Lima, E. C., Gomes, A. A., & Tran, H. N. (2020). Comparison of the nonlinear and linear forms of the van't Hoff equation for calculation of adsorption thermodynamic parameters (Δ S° andΔ H°). *Journal of Molecular Liquids*, 311, 113315.

Malik, P. K. (2003). Use of activated carbons prepared from sawdust and rice-husk for adsorption of acid dyes: a case study of Acid Yellow 36. *Dyes and Pigments*, 56(3), 239-249.

Moussavi, G., & Mahmoudi, M. (2009). Removal of azo and anthraquinone reactive dyes from industrial wastewaters using MgO nanoparticles. *Journal of Hazardous Materials*, 168(2-3), 806-812.

Mutunga, M. F., Wanyonyi, W. C., & Ongera, G. (2020). Utilization of Macadamia seed husks as a low-cost sorbent for removing cationic dye (basic blue 3 dye) from aqueous solution. *Environmental Chemistry and Ecotoxicology*, 2, 194-200.

Ofudje, E. A., Sodiya, E. F., Akinwunmi, F., Ogundiran, A. A.,

Oladeji, O. B., & Osideko, O. A. (2022). Eggshell derived calcium oxide nanoparticles for Toluidine blue removal. *Desalination of Water Treatment*, 247, 294–308

Ogundiran, A. A., Ofudje, E. A., Ogundiran, O. O., & Adewusi, A. M. (2022). Cationic dye adsorptions by eggshell waste: kinetics, isotherms and thermodynamics studies. *Desalination of Water Treatment*, 280, 157-167.

Olu-Owolabi, B. I., Adebowale, K. O., & Oseni, O. T. (2009). Physicochemical and thermodynamic adsorption studies of a ferric luvisol soil in Western Nigeria. *Soil and Sediment Contamination,* 19(1), 119-131.

Oyekanmi, A. A., Ahmad, A., Hossain, K., & Rafatullah, M. (2019). Adsorption of Rhodamine B dye from aqueous solution onto acid treated banana peel: Response surface methodology, kinetics and isotherm studies. *PLoS One*, 14(5), e0216878.

Qian, W. C., Luo, X. P., Wang, X., Guo, M., & Li, B. (2018). Removal of methylene blue from aqueous solution by modified bamboo hydrochar. *Ecotoxicology and Environmental Safety*, 157, 300-306.

Qin, Q., Ma, J. & Liu, K. (2009). Adsorption of anionic dyes on ammonium-functionalized MCM-41. *Journal of Hazardous Materials*, 162; 133–139.

Revellame, E. D., Fortela, D. L., Sharp, W., Hernandez, R., & Zappi, M. E. (2020). Adsorption kinetic modeling using pseudo-first order and pseudo-second order rate laws: A review. *Cleaner Engineering and Technology*, 1, 100032.

Reynier N., Coudert L., Blais J.F., Mercier G., & Besner S. (2015). Treatment of contaminated soil leachate by precipitation, adsorption and ion Exchange.

Journal of Environmental Chemistry Engineering, 3, 977–985.

Salleh, M. A. M., Mahmoud, D. K., Karim, W. A. W. A., & Idris, A. (2011). Cationic and anionic dye adsorption by agricultural solid wastes: a comprehensive review. *Desalination*, 280(1-3), 1-13.

Sharma, A., Siddiqui, Z. M., Dhar, S., Mehta, P., & Pathania, D. (2019). Adsorptive removal of congo red dye (CR) from aqueous solution by Cornulaca monacantha stem and biomass-based activated carbon: isotherm, kinetics and thermodynamics. *Separation science and echnology*, 54(6), 916-929.

Stjepanović, M., Velić, N., Galić, A., Kosović, I., Jakovljević, T., & Habuda-Stanić, M. (2021). From waste to biosorbent: Removal of congo red from water by waste wood biomass. *Water*, 13(3), 279.

Tunç, Ö., Tanacı, H., & Aksu, Z. (2009). Potential use of cotton plant wastes for the removal of Remazol Black B reactive dye. *Journal of Hazardous Materials*, 163(1), 187-198.

Yagub, M. T., Sen, T. K., Afroze, S., & Ang, H. M. (2014). Dye and its removal from aqueous solution by adsorption: a review. *Advances in colloid and interface science*, 209, 172-184.

Zhu M., Zhu L., Wang J., Yue T., Li R., & Li Z. (2017). Adsorption of Cd (II) and Pb (II) by in situ oxidized Fe3O4 membrane grafted on 316L porous stainless steel filter tube and its potential application for drinking water treatment. *Journal Environmental Management*, 196, 127–136.

Nigerian Journal of Science and Environment 2024 Volume 22 (2) 28 – 50 ISSN: 3043 – 4440
https://doi.org/10.61448/njse222243

Table I: Kinetic models parameters for CR adsorption on OP and ML

		Pseudo first order					Pseudo-second order			
	C_o(mg/L)	C_e (mg/L)	$Q_{e(exp)}$ (mg/g)	$Q_{e(cal)}$ (mg/g)	K_1	R^2	%SSE	$Q_{e(cal)}$ (mg/g)	K_2	R^2	%SSE
orange peel	50	23.31	21.36	18.21	0.136	0.922	0.044	20.13	0.014	0.988	0.017
	100	38.2	33.4	28.93	0.419	0.916	0.040	32.87	0.027	0.987	0.005
	150	65.4	48.22	50.02	0.481	0.937	0.011	47.37	0.039	0.978	0.005
	200	95.31	55.25	58.77	0.721	0.944	0.019	56.74	0.011	0.985	0.008
	250	117.18	61.12	65.38	0.881	0.928	0.021	60.26	0.126	0.988	0.004
mango leaf	50	32.41	25.33	24.115	0.113	0.957	0.014	19.45	0.052	0.926	0.07
	100	46.33	42.22	40.22	0.181	0.988	0.014	37.783	0.158	0.924	0.032
	150	75.4	54.34	53.37	0.201	0.977	0.005	49.322	0.298	0.969	0.028
	200	94.51	65.26	64.54	0.421	0.994	0.003	60.377	0.474	0.915	0.023
	250	116.12	73.41	71.11	0.671	0.995	0.009	69.215	0.625	0.927	0.017

Table II: Isotherm models parameters for CR adsorption onto OP and ML

Constants	orange peel (OP)	mango leaf (ML)
Langmuir isotherm		
Q_{max} (mg g^{-1})	64.23	70.64
R_L (L mg^{-1})	0.516	0.53
R^2	0.898	0.977
Freundlich isotherm		
1/n (L mg^{-1})	0.502	0.370
K_F (mg g^{-1})	48.116	34.63
R^2	0.998	0.958

Table III: Thermodynamic parameters for adsorption of CR

		OP		ML		
T℃	ΔG	ΔH	ΔS	ΔG	ΔH	ΔS
25	-1.42			-2.34		
30	-2.82			-3.56		
35	-3.49	6.87	1.244	-4.51	10.203	4.512
40	-3.87			-5.82		
45	-4.12			-6.76		